

ORIGINAL ARTICLE: EPIDEMIOLOGY,
CLINICAL PRACTICE AND HEALTH

Detection of changes in the locus coeruleus in patients with mild cognitive impairment and Alzheimer's disease: High-resolution fast spin-echo T1-weighted imaging

Junko Takahashi,¹ Toshihide Shibata,¹ Makoto Sasaki,² Masako Kudo,¹ Hisashi Yanezawa,¹ Satoko Obara,¹ Kohsuke Kudo,³ Kenji Ito,² Fumio Yamashita² and Yasuo Terayama¹

¹Department of Neurology and Gerontology, School of Medicine, ²Division of Ultrahigh Field MRI, Institute for Biomedical Sciences, Iwate Medical University, Morioka, and ³Department of Diagnostic and Interventional Radiology, Hokkaido University Hospital, Sapporo, Japan

Aim: Neuronal degeneration in the locus coeruleus occurs in the early phase of Alzheimer's disease, similar to mild cognitive impairment. The locus coeruleus produces norepinephrine, a deficiency of which causes both memory disturbance and psychological symptoms. Thus, we evaluated signal alterations in the locus coeruleus of patients with Alzheimer's disease and mild cognitive impairment using a high-resolution fast spin-echo T1-weighted imaging.

Methods: A total of 22 patients with Alzheimer's disease, 47 patients with mild cognitive impairment and 26 healthy controls were prospectively examined by high-resolution fast spin-echo T1-weighted imaging at 3 Tesla. Signal intensities in the locus coeruleus were manually measured and expressed relative to those in the adjacent white matter structures as contrast ratios.

Results: Locus coeruleus contrast ratios were significantly reduced in patient groups with Alzheimer's disease, mild cognitive impairment that converted to Alzheimer's disease and mild cognitive impairment that did not convert to Alzheimer's disease (1.80–16.09% [median, 9.30%], 3.45–14.84% [median 6.87%] and 3.01–19.19% [median 7.72%], respectively) compared with the healthy control group (6.24–20.94% [median 14.35%]; $P < 0.0001$). The sensitivity and specificity for discriminating these diseases were 85.0% and 69.2%, respectively, which suggests that this measurement can be carried out reliably. There was no significant difference in the locus coeruleus contrast ratios among the Alzheimer's disease, mild cognitive impairment-converted and mild cognitive impairment-non-converted groups.

Conclusions: High-resolution fast spin-echo T1-weighted imaging can show signal attenuation in the locus coeruleus of patients with Alzheimer's disease or with mild cognitive impairment whose pathology may or may not eventually convert to Alzheimer's disease. *Geriatr Gerontol Int* 2015; 15: 334–340.

Keywords: Alzheimer's disease, locus coeruleus, magnetic resonance imaging, mild cognitive impairment, neuromelanin.

Introduction

The locus coeruleus (LC) is a small, rod-shaped nucleus located in the pontine tegmentum (PT) along the lateral edge of the floor of the fourth ventricle. It contains noradrenergic neurons that send widespread projections throughout the central nervous system.^{1,2} LC neu-

ronal loss is one of the characteristic pathologies of early-stage Parkinson's disease (PD) and Alzheimer's disease (AD).^{3–8} Detection of LC degeneration by neuroimaging could therefore contribute to the early or preclinical diagnosis of AD facilitating the use of disease-modifying interventions in the future. However, conventional magnetic resonance imaging (MRI) has not been successful in delineating the LC. Recently, visualization of neuromelanin-containing nuclei, such as the LC and substantia nigra pars compacta (SNc), has become possible through the introduction of a fast spin-echo (FSE) T1-weighted image^{9,10} that can enhance T1-related contrast of neuromelanin.^{11,12} Using this

Accepted for publication 2 February 2014.

Correspondence: Dr Junko Takahashi, MD, Department of Neurology and Gerontology, Iwate Medical University, 19-1 Uchimarui, Morioka, Japan. Email: jtkahas@iwate-med.ac.jp

method, signal attenuation or volume loss in the SNc and/or LC detected in patients with PD, various parkinsonisms and depression, results that might reflect pathological or functional changes in these nuclei.^{9,13,14} However, changes in the LC of patients with AD or mild cognitive impairment (MCI) have not yet been investigated. Thus, we attempted to determine: (i) whether high-resolution FSE T1-weighted MRI can detect changes in the LC of patients with AD and MCI; and (ii) if this method can in fact predict the progression of MCI to AD.

Methods

Patients

MRI was prospectively carried out between 1 November 2006 and 31 December 2011 in the Department of Neurology and Gerontology, School of Medicine, Iwate Medical University, Morioka, Japan. Participants were 22 consecutive patients with AD who met the criteria for probable AD according to The National Institute of Neurological and Communicative Diseases and Stroke and Alzheimer's Disease and Related Disorders Association^{15,16} and Functional Assessment Staging (FAST) Stage 4 (11 men and 11 women; age 59–86 years [median 76.5 years]; duration of disease 0.5–10 years [median 5 years]), and 47 consecutive patients with amnesic MCI who fulfilled Petersen's criteria^{17,18} and FAST Stage 3 criteria (22 men and 25 women; age 60–87 years [median 73 years]; duration of disease, 0.5–7 years [median 2 years]). Scores on the Mini-Mental State Examination (MMSE) carried out within 1 week of the MR examination were 16–26 (median 22) in patients with AD and 19–30 (median 25) in patients with MCI. A total of 15 out of the 22 patients with AD and 25 out of the 47 patients with MCI were given cholinesterase inhibitors. Additionally, 26 healthy elderly individuals with no known neurological disorders (12 men, 14 women; age 60–83 years [median 70 years]) were also examined. These 26 control subjects had no abnormal neurological findings and their MR T2-weighted images were normal.

After being observed for at least 2 years (2–6 years [median 4 years]), 18 patients with MCI (8 men and 10 women; age 62–85 years [median 73 years]) met the criteria for probable AD according to the The National Institute of Neurological and Communicative Diseases and Stroke and Alzheimer's Disease and Related Disorders Association. These patients were then included in the AD-converted MCI (MCIC) group. A total of 20 patients who did not meet the criteria for probable AD (8 men and 12 women; age 60–87 years [median 74 years]) were included in the non-converted MCI (MCInc) group. The remaining nine patients with MCI were excluded from the study; one patient showed

reversion of symptoms, and eight patients stopped visiting the hospital.

We carried out all examinations after obtaining both the approval of the Iwate Medical University Research Ethics Committee and after obtaining written informed consent from each participant.

Imaging protocol

Using a 3-Tesla MR scanner (Signa Excite HDxt; GE Healthcare, Milwaukee, WI, USA), we obtained oblique axial FSE T1-weighted images (repetition time 600 ms; echo time 14 ms; flip angle 90 degrees; echo train length 2; number of excitations 8; matrix size 512 × 320; field of view 220 mm; pixel size 0.42 × 0.68 mm; number of slices 10; slice thickness 2.5 mm; interslice gap 1 mm; acquisition time 12 min) as previously reported.^{9,10} Images were carefully set perpendicular to the fourth ventricle floor, with coverage between the posterior commissure and the inferior border of the pons. T1- and T2-weighted images of the entire brain were also obtained from all participants in order to exclude the possibility of other neurological disorders, and to confirm the absence of coexisting lesions, such as discrete cerebral infarcts and hemorrhages, that could interfere with further assessment.

Data processing

For quantitative evaluation of the high-resolution FSE T1-weighted image, signal intensities were measured using circular regions of interest (ROI) of 1 mm² and 10 mm² for the LC and PT, respectively. ROI were viewed on a liquid crystal display in the section through the upper pons (Fig. 1a). One of the authors (J T), who was blind to subject information, measured the signal intensity of the LC at 7 mm below the section through the inferior edge of the inferior colliculus. Three measurements were carried out at 1-week intervals, and the obtained values were then averaged. The ROI of the LC was manually derived using the highest intensity position around the floor of the fourth ventricle. LC contrast ratios (LC-CR) were calculated using the following equation: $LC-CR = (SI_{LC} - SI_{PT}) / SI_{PT}$, where SI_{LC} is the averaged signal intensity the left and right LC, and SI_{PT} is the signal intensity of the PT.

For evaluating mesial temporal atrophy, interuncal distance (IUD) was measured bilaterally from the section intersecting the uncus on the T1-weighted image, as previously reported.¹⁹ The measurements were carried out a total of three times with 1-week intervals between measurements, after which the measured values were averaged.

Statistical analyses

Kruskal–Wallis and Steel–Dwass tests were used to determine differences in LC-CR among the AD, MCIC,

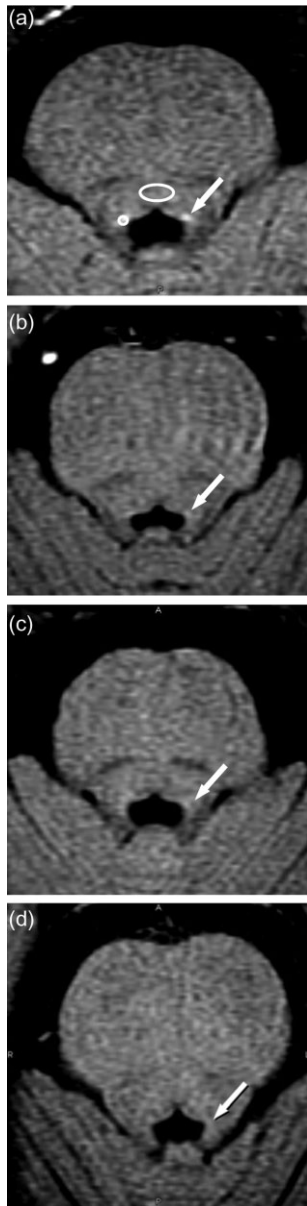


Figure 1 High-resolution fast spin-echo T1-weighted imaging of a healthy subject, patients with mild cognitive impairment (MCI) and a patient with Alzheimer's disease (AD). (a) A healthy subject. (b) A patient with MCI without conversion to AD (MCInc). (c) A patient with MCI converted to AD (MCIc). (d) A patient with AD. (a) In the healthy subject, a punctate region of high signal intensity showing the locus coeruleus (LC) is evident (arrow), (b–d) whereas the signal intensity is remarkably diminished in patients with MCInc, MCIc, or AD (arrows). Small circle, region of interest for measuring signal intensity in the LC (1 mm²); large circle, region of interest for the pontine tegmentum (10 mm²).

MCInc and control groups. These tests were also carried out to evaluate differences in participant demographics among the groups. To determine the sensitivity and specificity of high-resolution FSE T1-weighted

imaging for discriminating among the four groups, receiver operating characteristic (ROC) analyses were carried out. Cut-off values were determined by the Youden index. Multiple regression analysis was also used to examine whether the demographics were independently related to LC-CR. Intraoperator agreement of the obtained measurements was determined by calculating the intraclass correlation coefficient (ICC). The alpha level for all analyses was 0.05.

Results

MR examination was successfully carried out for all participants without significant motion artifact, and the images obtained were eligible for further quantitative analyses. Patient demographics are shown in Table 1. No significant differences in sex or administration of cholinesterase inhibitors were observed among the groups. Several observations were made: the healthy subjects were younger than patients with AD ($P = 0.042$, Steel–Dwass test); disease durations were significantly longer in patients with AD than in patients with MCIc and MCInc ($P = 0.045$ and 0.008 , respectively; Steel–Dwass test); MMSE scores were significantly lower in patients with AD than in patients with MCInc ($P < 0.0002$, Steel–Dwass test); and IUDs were significantly larger in the AD group than in the control group ($P = 0.0024$, Steel–Dwass test). However, none of these demographic parameters was correlated with the LC-CR. Similarly, treatment with cholinesterase inhibitors was not correlated with the LC-CR ($P = 0.5724$, Steel–Dwass test). The correlation coefficients describing a lack of association between LC-CR and age, disease duration, MMSE, sex and cholinesterase inhibitor medication were $r = 0.022$ ($P = 0.835$), $r = -0.049$ ($P = 0.700$), $r = -0.027$ ($P = 0.834$), $r = 0.064$ ($P = 0.0548$) and $r = 0.026$ ($P = 0.843$), respectively.

LC-CR ranged from 1.80–16.09% (median 9.30%), 3.45–14.84% (median 6.87%), 3.01–19.19% (median 7.72%) and 6.24–20.94% (median 14.35%) in the AD, MCIc, MCInc, and control groups, respectively. A significant difference was observed among the groups ($P < 0.0001$) using the Kruskal–Wallis test.

Additional analysis using the Steel–Dwass test showed that the LC-CR were markedly decreased in the AD, MCIc and MCInc groups ($P = 0.0031$, 0.0002 , and 0.0168 , respectively) compared with the healthy control group (Fig. 2), whereas no significant differences were observed among the AD, MCIc and MCInc groups ($P = 0.45$ – 1.00).

ROC analyses showed that the area under the ROC curve (AUC) of the LC-CR for discriminating the AD and MCI groups from the healthy control group was 0.83, and the sensitivity and specificity were 85.0% and 69.2%, respectively, when the cut-off value was set at

Table 1 Demographics of patients with Alzheimer's disease, patients with mild cognitive impairment and healthy individuals

		AD (n = 22)	MCIc (n = 18)	MCInc (n = 20)	Control (n = 26)	P-value [†]
Age (years)	Range (median)	59–86 (76.5)	62–85 (73)	60–87 (75)	60–83 (70)*	0.027
Sex	Men (%)	11 (50)	8 (44)	8 (40)	12 (46)	0.93
Duration (years)	Range (median)	0.5–10 (5)**	0.5–7 (2)	0.5–7 (2)	NA	0.005
MMSE	Range (median)	16–26 (22)**	19–28 (25)	19–30 (26)	NA	<0.001
CE inhibitors	Number (%)	15 (68)	10 (56)	15 (75)	NA	0.37
IUD (mm)	Range (median)	23.2–33.5 (27.9)**	19.0–31.1 (26.2)	20.8–33.5 (24.9)	19.1–31.0 (25.3)	0.004

* $P < 0.05$, ** $P < 0.01$ (Steel–Dwass test); [†]Kruskal–Wallis test. AD, Alzheimer's disease; CE, cholinesterase; IUD, interuncal distance; MCIc, mild cognitive impairment converter; MCInc, mild cognitive impairment non-converter; MMSE, Mini-Mental State Examination; NA, not applicable.

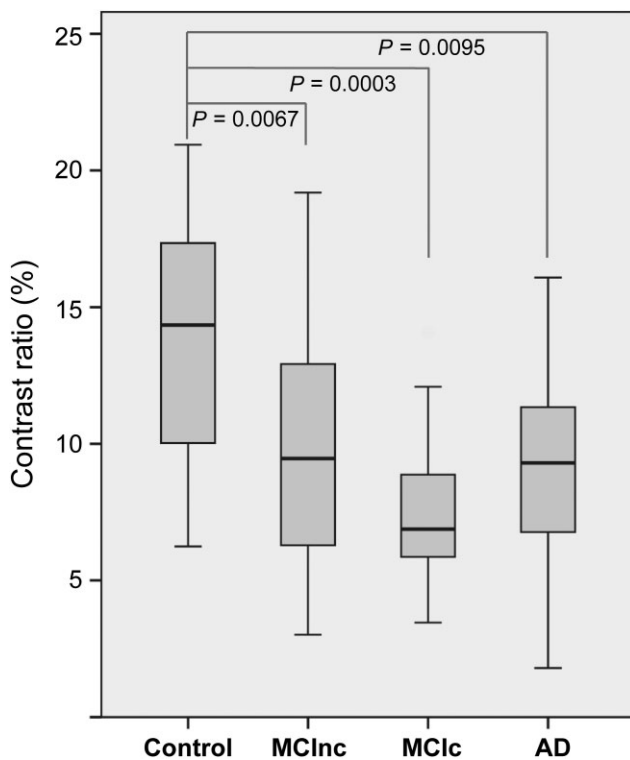


Figure 2 Locus coeruleus contrast ratios in healthy subjects and in patients with mild cognitive impairment (MCI) or with Alzheimer's disease (AD). The locus coeruleus contrast ratio was markedly decreased in the MCI without conversion to AD (MCInc), MCI converted to AD (MCIc) and AD groups than in the healthy control group, whereas no significant difference was observed between the AD, MCIc and MCInc groups.

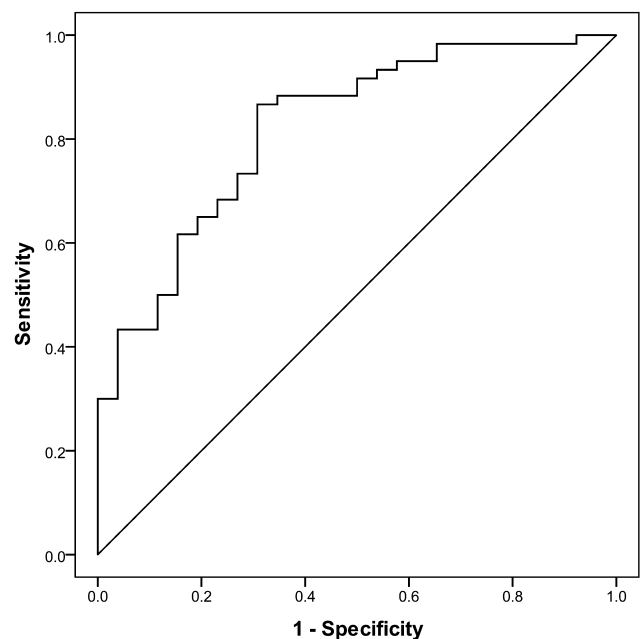


Figure 3 Receiver operating characteristic curves of the locus coeruleus contrast ratio in patients with Alzheimer's disease, mild cognitive impairment and normal control group.

12.5% (Fig. 3). In contrast, the AUC for discriminating the AD and MCIc groups from the MCInc and healthy control groups was 0.69, and the sensitivity and specificity were 63.4% and 67.4%, respectively, with a cut-off value of 9.18%.

ICC values for the manual measurements of LC were 0.984–0.997, showing excellent intraoperator agreement.

Discussion

In the present study, we successfully detected signal attenuations in the LC of patients with AD or MCI using high-resolution FSE T1-weighted imaging. This finding corresponds well to pathological findings of a decrease in neuromelanin contents as a result of neuronal loss in the LC of these patients. Thus, high-resolution FSE T1-weighted imaging could enable direct visualization of the LC degeneration, which occurs in AD and MCI, a progression that cannot be detected by other MRI techniques.

We observed that signal attenuation in the LC was evident even in patients with MCI; furthermore, there were no substantial differences in signal changes between the MCI and AD groups. Noticeably, this relative stability of the LC signal differs from what is observed in mesial temporal lobe atrophy. Atrophy of mesial temporal lobe structures, such as the hippocampus, entorhinal cortex and amygdala, tends to follow AD progression.^{20,21} In the present study, IUD, which reflects mesial temporal lobe atrophy, gradually increased along with disease severity, and showed no substantial correlation with LC changes.

Pathological changes of the LC in AD and MCI have been thoroughly investigated. AD is characterized by two pathological hallmarks: extracellular amyloid deposits^{22,23} and intraneuronal neurofibrillary tangles as a result of phosphorylated tau.²² Amyloid beta deposits are first observed in the neocortex, then in the hippocampal formation, subcortical regions and finally in several brainstem nuclei.^{22,23} Hence, amyloid beta deposits in the LC are not detectable until the disease has progressed significantly. In contrast, the deposition of phosphorylated tau and subsequent neuronal loss in the LC are observed from very early stages of AD, MCI and preclinical AD.^{3,6,24–27} However, no investigators have previously carried out an *in vivo* evaluation of alterations in the LC of patients with AD or MCI, mainly because the LC has been an “invisible” structure on conventional MR images. Thus, signal attenuation in the LC, observed using high-resolution FSE T1-weighted imaging, could comprise an effective marker for the detection of early or prodromal stages of AD.

Contrary to our expectations, we observed significant signal attenuation in the LC not only in the MCIC group, but also in the MCInc group, with no substantial differences being observed between these two groups. These results suggest that signal changes in the LC are not specific to the prodromal stage of AD and cannot predict whether patients with MCI will convert to AD. However, conversion to AD can be predicted by quantitative assessment of mesial temporal lobe atrophy using sophisticated voxel-based morphometry (VBM) techniques.^{20,21,28}

MCI can result from a number of heterogeneous causes, such as dementia with diffuse Lewy bodies, PD dementia and argyrophilic grain dementia.²⁹ Neuronal loss in the LC was reported in several pathological studies on these disorders,^{7,30–32} consistent with the LC signal changes seen in the MCInc group in the present study. Thus, the present results suggest that neuronal loss in the LC might be one of the cardinal mechanisms of MCI. Furthermore, we could not distinguish MCI that converted to AD from MCI that did not convert to AD by using this method.

In considering alternative artifactual interpretations of these data, we can make note of several previous observations. According to a report by Kaneda, in patients who have had gadolinium, high signal intensity might be observed.³³ However, the present patients and participants had not used gadolinium. Manganese is a heavy metal that also produces high-intensity signals in T1-weighted images. The causes of manganese deposition in the brain are hepatic encephalopathy and intravenous hyperalimentation. In the present study, none of the participants and patients had experienced these conditions.

Conversely, iron shows low intensity on T2-weighted imaging of the brain. In contrast, iron generally produced no changes in high-resolution FSE T1-weighted imaging. For example, although the red nucleus contains a relatively large component of iron, it did not show high intensity using this sequence.

The present study had several limitations. First, we did not compare LC changes with other biomarkers for LC-related norepinephrine dysfunction, such as norepinephrine concentration in the cerebrospinal fluid. Second, the present study could not show whether LC signal changes are present in non-AD dementias. In this study, we observed patients in the MCInc group for 2–6 years, which was too short a period to determine the final clinical diagnosis of these patients. Third, this study did not elucidate advantages of this method over VBM or other sophisticated quantitative methods except by comparing LC changes with IUD, a marker classically used to reflect medial temporal lobe atrophy. In the present study, we did not obtain 3-D T1-weighted images, which are primarily used for VBM, or T1 coronal images because of a limited examination time schedule. Direct comparison between high-resolution FSE T1-weighted imaging and VBM is required to compare the diagnostic validity of these two methods.

There are several disadvantages of the technique used for T1-weighted FSE imaging in the present study. The technique is time-consuming, has relatively low spatial resolution for assessment of the LC and suffers from substantial signal heterogeneity as a result of the heterogeneous local magnetic field at 3 Tesla, which can diminish the quantitative value of these measurements.

The manual measurement we carried out might also possibly explain the large variability in measures, although intraoperator agreement was high in this study. Although all patients had mild symptoms and could finish examinations without significant motion artifact, there were some effects of cardiac cycle and cerebrospinal fluid flow dynamics.³⁴ Three-dimensional imaging techniques and automatic measurements are required to improve the precision of measurements of signal alterations in the LC.³⁵ We are currently using these techniques in our ongoing studies.

The present study showed that high-resolution FSE T1-weighted imaging enables visualization of signal attenuation in the LC of patients with AD or MCI. However, it remains unknown whether this technique can be used to detect changes in patients with preclinical AD. It is also unclear whether the LC signal can track the progression of AD symptoms or predict patient outcomes. We assessed the MCI patients as converter/non-converter by evaluating only the symptoms. Therefore, longitudinal evaluations of MR images and point-by-point analyses are required to clarify these issues. High-resolution FSE T1-weighted imaging shows significant signal attenuation in the LC of patients with AD and MCI, with or without conversion to AD, indicating that neuronal loss can occur early on in these patients.

Acknowledgements

Our deepest appreciation goes to the late Dr Satoshi Takahashi, who made an inspirational effort in leading our study during his short life. This work was partly supported by a Grant-in-Aid for Strategic Medical Science Research from the Ministry of Education, Culture, Sport, Science and Technology of Japan.

Disclosure statement

The authors declare no conflict of interest.

References

- 1 Aston-Jones G, Cohen JD. An integrative theory of locus coeruleus-norepinephrine function: adaptive gain and optimal performance. *Annu Rev Neurosci* 2005; **28**: 403–450.
- 2 Berridge CW, Waterhouse BD. The locus coeruleus-noradrenergic system: modulation of behavioral state and state-dependent cognitive processes. *Brain Res Brain Res Rev* 2003; **42**: 33–84.
- 3 Braak H, Del Tredici K. Alzheimer's pathogenesis: is there neuron-to-neuron propagation? *Acta Neuropathol (Berl)* 2011; **121**: 589–595.
- 4 Braak H, Del Tredici K, Rub U, de Vos RA, Jansen Steur EN, Braak E. Staging of brain pathology related to sporadic Parkinson's disease. *Neurobiol Aging* 2003; **24**: 197–211.
- 5 Braak H, Rub U, Del Tredici K. Cognitive decline correlates with neuropathological stage in Parkinson's disease. *J Neurol Sci* 2006; **248**: 255–258.
- 6 Braak H, Thal DR, Ghebremedhin E, Del Tredici K. Stages of the pathologic process in Alzheimer disease: age categories from 1 to 100 years. *J Neuropathol Exp Neurol* 2011; **70**: 960–969.
- 7 Del Tredici K, Braak H. Dysfunction of the locus coeruleus-norepinephrine system and related circuitry in Parkinson's disease-related dementia. *J Neurol Neurosurg Psychiatry* 2013; **84**: 774–783.
- 8 Szot P. Common factors among Alzheimer's disease, Parkinson's disease, and epilepsy: possible role of the noradrenergic nervous system. *Epilepsia* 2012; **53** (Suppl 1): 61–66.
- 9 Sasaki M, Shibata E, Tohyama K *et al*. Neuromelanin magnetic resonance imaging of locus coeruleus and substantia nigra in Parkinson's disease. *Neuroreport* 2006; **17**: 1215–1218.
- 10 Shibata E, Sasaki M, Tohyama K *et al*. Age-related changes in locus coeruleus on neuromelanin magnetic resonance imaging at 3 Tesla. *Magn Reson Med Sci* 2006; **5**: 197–200.
- 11 Enochs WS, Petherick P, Bogdanova A, Mohr U, Weissleder R. Paramagnetic metal scavenging by melanin: MR imaging. *Radiology* 1997; **204**: 417–423.
- 12 Tosk JM, Holshouser BA, Aloia RC *et al*. Effects of the interaction between ferric iron and L-dopa melanin on T1 and T2 relaxation times determined by magnetic resonance imaging. *Magn Reson Med* 1992; **26**: 40–45.
- 13 Shibata E, Sasaki M, Tohyama K *et al*. Use of neuromelanin-sensitive MRI to distinguish schizophrenic and depressive patients and healthy individuals based on signal alterations in the substantia nigra and locus coeruleus. *Biol Psychiatry* 2008; **64**: 401–406.
- 14 Shibata E, Sasaki M, Tohyama K, Otsuka K, Sakai A. Reduced signal of locus coeruleus in depression in quantitative neuromelanin magnetic resonance imaging. *Neuroreport* 2007; **18**: 415–418.
- 15 Dubois B, Feldman HH, Jacova C *et al*. Research criteria for the diagnosis of Alzheimer's disease: revising the NINCDS-ADRDA criteria. *Lancet Neurol* 2007; **6**: 734–746.
- 16 McKhann G, Drachman D, Folstein M, Katzman R, Price D, Stadlan EM. Clinical diagnosis of Alzheimer's disease: report of the NINCDS-ADRDA Work Group under the auspices of Department of Health and Human Services Task Force on Alzheimer's Disease. *Neurology* 1984; **34**: 939–944.
- 17 Petersen RC, Stevens JC, Ganguli M, Tangalos EG, Cummings JL, DeKosky ST. Practice parameter: early detection of dementia: mild cognitive impairment (an evidence-based review). Report of the Quality Standards Subcommittee of the American Academy of Neurology. *Neurology* 2001; **56**: 1133–1142.
- 18 Winblad B, Palmer K, Kivipelto M *et al*. Mild cognitive impairment—beyond controversies, towards a consensus: report of the International Working Group on Mild Cognitive Impairment. *J Intern Med* 2004; **256**: 240–246.
- 19 Saka E, Dogan EA, Topcuoglu MA, Senol U, Balkan S. Linear measures of temporal lobe atrophy on brain magnetic resonance imaging (MRI) but not visual rating of white matter changes can help discrimination of mild cognitive impairment (MCI) and Alzheimer's disease (AD). *Arch Gerontol Geriatr* 2007; **44**: 141–151.
- 20 Matsuda H, Mizumura S, Nemoto K *et al*. Automatic voxel-based morphometry of structural MRI by SPM8 plus diffeomorphic anatomic registration through

- exponentiated lie algebra improves the diagnosis of probable Alzheimer Disease. *AJNR Am J Neuroradiol* 2012; **33**: 1109–1114.
- 21 Whitwell JL, Przybelski SA, Weigand SD *et al.* 3D maps from multiple MRI illustrate changing atrophy patterns as subjects progress from mild cognitive impairment to Alzheimer's disease. *Brain* 2007; **130**: 1777–1786.
 - 22 Braak H, Braak E. Neuropathological staging of Alzheimer-related changes. *Acta Neuropathol (Berl)* 1991; **82**: 239–259.
 - 23 Thal DR, Rub U, Orantes M, Braak H. Phases of A beta-deposition in the human brain and its relevance for the development of AD. *Neurology* 2002; **58**: 1791–1800.
 - 24 German DC, Manaye KF, White CL, 3rd *et al.* Disease-specific patterns of locus coeruleus cell loss. *Ann Neurol* 1992; **32**: 667–676.
 - 25 Grudzien A, Shaw P, Weintraub S, Bigio E, Mash DC, Mesulam MM. Locus coeruleus neurofibrillary degeneration in aging, mild cognitive impairment and early Alzheimer's disease. *Neurobiol Aging* 2007; **28**: 327–335.
 - 26 Huglund M, Sjöbeck M, Englund E. Locus ceruleus degeneration is ubiquitous in Alzheimer's disease: possible implications for diagnosis and treatment. *Neuropathology* 2006; **26**: 528–532.
 - 27 Zarow C, Lyness SA, Mortimer JA, Chui HC. Neuronal loss is greater in the locus coeruleus than nucleus basalis and substantia nigra in Alzheimer and Parkinson diseases. *Arch Neurol* 2003; **60**: 337–341.
 - 28 Yoshiura T, Hiwatashi A, Yamashita K *et al.* Deterioration of abstract reasoning ability in mild cognitive impairment and Alzheimer's disease: correlation with regional grey matter volume loss revealed by diffeomorphic anatomical registration through exponentiated lie algebra analysis. *Eur Radiol* 2011; **21**: 419–425.
 - 29 Saito Y. Neuropathology of mild cognitive impairment. *Neuropathology* 2007; **27**: 578–584.
 - 30 Bosboom JL, Stoffers D, Wolters E. Cognitive dysfunction and dementia in Parkinson's disease. *J Neural Transm* 2004; **111**: 1303–1315.
 - 31 Jellinger KA. Alpha-synuclein pathology in Parkinson's and Alzheimer's disease brain: incidence and topographic distribution – a pilot study. *Acta Neuropathol (Berl)* 2003; **106**: 191–201.
 - 32 McMillan PJ, White SS, Franklin A *et al.* Differential response of the central noradrenergic nervous system to the loss of locus coeruleus neurons in Parkinson's disease and Alzheimer's disease. *Brain Res* 2011; **1373**: 240–252.
 - 33 Kaneda T. High Signal Intensity in the Dentate Nucleus and Globus Pallidus on Unenhanced T1-weighted MR Images: Relationship with Increasing Cumulative Dose of a Gadolinium-based Contrast Material. 2013.
 - 34 Keren NI, Lozar CT, Harris KC, Morgan PS, Eckert MA. In vivo mapping of the human locus coeruleus. *Neuroimage* 2009; **47**: 1261–1267.
 - 35 Keren NI, Lozar CT, Harris KC, Morgan PS, Eckert MA. In vivo mapping of the human locus coeruleus. *Neuroimage* 2009; **47**: 1261–1267.